

STREAKING ARTIFACTS REDUCTION FOR QSM

Hongjiang Wei¹, Wei Li², Nian Wang¹, and Chunlei Liu^{1,3}

¹Brain Imaging and Analysis Center, Duke University, Durham, NC, United States, ²University of Texas Health Science Center at San Antonio, TX, United States,

³Department of Radiology, School of Medicine, Duke University, Durham, NC, United States

INTRODUCTION: Quantifying susceptibility from the phase image is hampered by the ill-posed dipole filter inversion problem when $\mathbf{k}^2 - 3\mathbf{k}_z^2 = 0$ in the k-space [1]. The imperfect inversion on and near the conical surface results in streaking artifacts in the computed susceptibility maps. In this study, we introduced a novel image-space weighting function to suppress errors induced by imperfect phase measurement and unwrapping. This weighting function is applied in a joint L1 and L2 norm minimization procedure which can be solved rapidly using SPARSA solver. A significantly lower level of streaking artifacts is observed in the resulting susceptibility maps. The results are comparable to those obtained from COSMOS method [2], and the computation time for the reconstruction is less than one minute for a matrix size of 320×320×204.

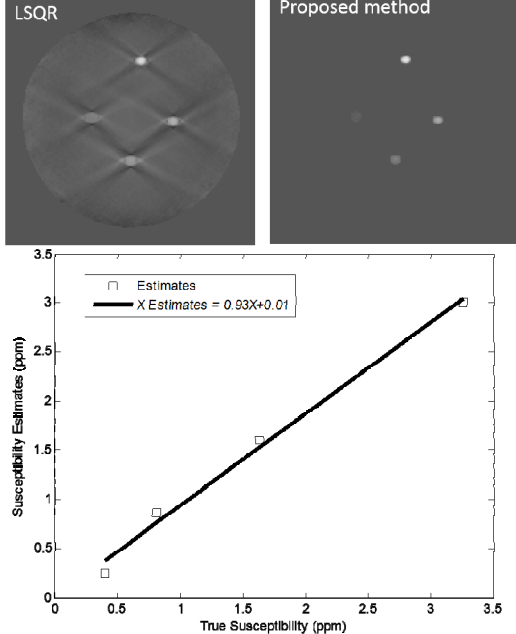


Fig. 1. (a) Comparison of the susceptibility maps of a phantom between LSQR and the proposed methods. (b) The increasing contrast with increasing gadolinium concentration.

calculations were performed on a desktop computer with an Intel Core i7-4770 TM CPU and 16GB RAM.

RESULTS: In Fig. 1, the calculated susceptibility maps of a phantom from LSQR [5] and the proposed method are compared. The

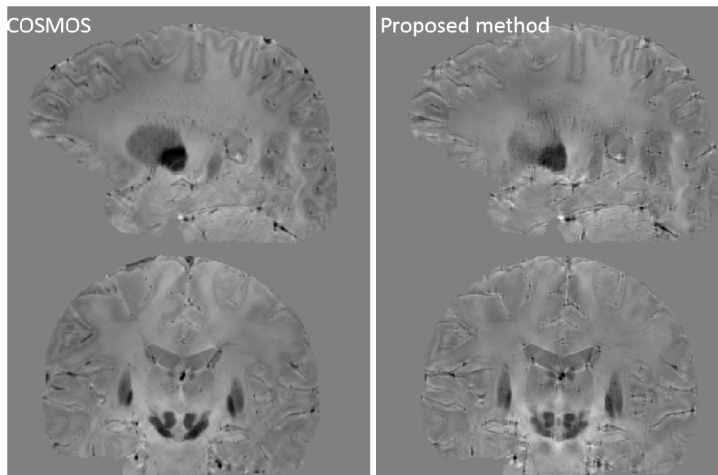


Fig. 2. Comparison of the susceptibility maps of human brain between COSMOS and the proposed reconstruction methods.

regions. Moreover, compared to the LSQR and COSMOS method, another significant improvement is the very fast computation, which is very suitable for 3D QSM reconstruction applications. **REFERENCES:** 1. de Rochefort L et al, Magn Reson Med., 2010; 63: 194-206. 2. Liu T et al, Magn Reson Med., 2009; 61(1): 196-204. 3. Stephan J et al, IEEE Trans Signal Processing, 2009; 57:2479-2493. 4. Li W et al, NMR Biomed., 2014; 27(2): 219-227. 5. Li W et al, Neuroimage, 2011; 55: 1645-1656.

METHODS: In this study, the image-space weighting was added for suppressing the streaking artifacts around the strong susceptibility sources. The proposed method essentially solves the following equation:

$$\chi = \min \left\{ \left\| W_{\text{Image}} (F^{-1} D_2 \cdot F \chi - \varphi) \right\|_2 + \beta_1 \cdot \| W \cdot G \cdot \chi \|_1 \right\} \quad [1]$$

φ is the filtered phase and χ is the unknown susceptibility maps. F and F^{-1} are Fourier transform and inverse Fourier transform, respectively. D_2 is the dipole kernel. The L1 norm computes the total variation of the gradient. β_1 is the penalty term. W_{Image} is the image-space weighting term. The image weights W_{Image} are estimated using the following equations:

$$\begin{cases} W_{\text{Image}} = 1, |\Delta\varphi| < \Delta\varphi_{\min} \\ W_{\text{Image}} = [\Delta\varphi_{\max} - |\Delta\varphi|] / [\Delta\varphi_{\max} - \Delta\varphi_{\min}], \Delta\varphi_{\min} < |\Delta\varphi| < \Delta\varphi_{\max} \\ W_{\text{Image}} = 0, \Delta\varphi_{\max} < |\Delta\varphi| \end{cases} \quad [2]$$

where the L1 norm of the gradient or total variation term is given by:

$$\| W \cdot G \cdot \chi \|_1 = \sqrt{(W_{Gx} \cdot G_x \cdot \chi)^2 + (W_{Gy} \cdot G_y \cdot \chi)^2 + (W_{Gz} \cdot G_z \cdot \chi)^2} \quad [3]$$

The W_{Gx} , W_{Gy} , W_{Gz} are derived using the invert-sign estimates for brain tissue without very large susceptibility variations. Eq. 1 can be solved iteratively using a SPARSA solver [3] for the proposed method. In this study, wrapped phase was unwrapped using Laplacian-based phase unwrapping method and the background phase was then removed using the proposed HARPERELLA method [4]. A cylindrical phantom with known susceptibility distributions was constructed with susceptibilities of 0.4, 0.81, 1.63, and 3.26 ppm. The

calculations were performed on a desktop computer with an Intel Core i7-4770 TM CPU and 16GB RAM. The susceptibility map calculated using LSQR method shows severe streaking artifact. However, the susceptibility maps calculating from the proposed method are essentially free of streaking artifacts. The results calculated using the proposed method show strong agreement with ground truth susceptibility values. The standard errors for each concentration is 10%, 2.5%, 3%, and 3%, respectively. The increase in susceptibility as a function of gadolinium concentration can be seen in coronal view. Fig. 2 shows that the results of a human brain are highly consistent with that of COSMOS. The streaking artifacts are removed and the susceptibility map allows excellent contrast between different tissues. For this particular dataset with a matrix size of 320×320×204, the reconstruction time for susceptibility maps is around 50 seconds for the proposed method.

CONCLUSIONS: We compared the susceptibility maps of a phantom obtained from LSQR method and a proposed streaking artifact reduction method. The proposed method leads to a significantly reduced level of streaking artifacts. The susceptibility maps of the COSMOS and the proposed methods are also compared. The proposed method is robust and produces susceptibility maps of a satisfactory level of contrast in different